

# UCSF

## UC San Francisco Previously Published Works

### Title

Combined Alloreactive CTL Cellular Therapy with Prodrug Activator Gene Therapy in a Model of Breast Cancer Metastatic to the Brain

### Permalink

<https://escholarship.org/uc/item/3xn1r47h>

### Journal

Clinical Cancer Research, 19(15)

### ISSN

1078-0432

### Authors

Hickey, Michelle J  
Malone, Colin C  
Erickson, Kate L  
[et al.](#)

### Publication Date

2013-08-01

### DOI

10.1158/1078-0432.ccr-12-3735

Peer reviewed



Published in final edited form as:

Clin Cancer Res. 2013 August 1; 19(15): 4137–4148. doi:10.1158/1078-0432.CCR-12-3735.

## Combined Alloreactive CTL Cellular Therapy with Prodrug Activator Gene Therapy in a Model of Breast Cancer Metastatic to the Brain

Michelle J. Hickey<sup>1</sup>, Colin C. Malone<sup>1</sup>, Kate L. Erickson<sup>1</sup>, Amy Lin<sup>1,\*</sup>, Horacio Soto<sup>1</sup>, Edward T. Ha<sup>1</sup>, Shuichi Kamijima<sup>2</sup>, Akihito Inagaki<sup>2</sup>, Masamichi Takahashi<sup>2</sup>, Yuki Kato<sup>3</sup>, Noriyuki Kasahara<sup>2,3,\*\*</sup>, Barbara M. Mueller<sup>4,\*\*</sup>, and Carol A. Kruse<sup>1,\*\*</sup>

<sup>1</sup>Department of Neurosurgery, University of California Los Angeles, Los Angeles, CA 90095

<sup>2</sup>Department of Medicine, University of California Los Angeles, Los Angeles, CA 90095

<sup>3</sup>Department of Molecular & Medical Pharmacology, University of California Los Angeles, Los Angeles, CA 90095

<sup>4</sup>Torrey Pines Institute for Molecular Studies, San Diego, CA 92121

### Abstract

**Purpose**—Individual or combined strategies of cellular therapy with alloreactive cytotoxic T lymphocytes (alloCTL) and gene therapy employing retroviral replicating vectors (RRV) encoding a suicide prodrug activating gene were explored for the treatment of breast tumors metastatic to the brain.

**Experimental Design**—AlloCTL, sensitized to the human leukocyte antigens of MDA-MB-231 breast cancer cells, were examined *in vitro* for anti-tumor functionality toward breast cancer targets. RRV encoding the yeast cytosine deaminase (CD) gene was tested *in vivo* for virus spread, ability to infect, and kill breast cancer targets when exposed to 5-fluorocytosine (5-FC). Individual and combination treatments were tested in subcutaneous and intracranial xenograft models with 231BR, a brain tropic variant.

**Results**—AlloCTL preparations were cytotoxic, proliferated and produced interferon-gamma when coincubated with target cells displaying relevant HLA. *In vivo*, intratumorally-placed alloCTL trafficked through one established intracranial 231BR focus to another in contralateral brain and induced tumor cell apoptosis. RRV-CD efficiently spread *in vivo*, infected 231BR and induced their apoptosis upon 5-FC exposure. Subcutaneous tumor volumes were significantly reduced in alloCTL and/or gene therapy treated groups compared to control groups. Mice with established intracranial 231BR tumors treated with combined alloCTL and RRV-CD had a median survival of 97.5 days compared with single modalities (50–83 days); all experimental treatment

Correspondence to: Carol A. Kruse, PhD, UCLA Department of Neurosurgery, 695 Charles E. Young Drive, South, Gonda 1554B, Mail Code 176122, Los Angeles, CA, 90095, Phone: 310-267-2535, ckruse@mednet.ucla.edu.

\*current address: Amy Lin, Ph.D., Tocagen, Inc. 3030 Bunker Hill Street, Ste #230, San Diego, CA 92109, alin@tocagen.com

\*\*These authors jointly participated in oversight of this research.

Disclosure of Potential Conflicts of Interest: No conflicts to declare by all authors.

#### Authors' Contributions

**Conception, design, and study supervision:** N. Kasahara, B.M. Mueller, C.A. Kruse

**Development of methodology:** M.J. Hickey, A. Lin, N. Kasahara, B.M. Mueller, C.A. Kruse

**Acquisition of data/technical support, data presentation:** C.C. Malone, K.L. Erickson, H. Soto, E.T. Ha, Y. Kato, S. Kamijima, A. Inagaki, M. Takahashi, A. Lin

**Data analysis and interpretation, statistical review and writing:** M.J. Hickey, N. Kasahara, B.M. Mueller, C.A. Kruse

groups survived significantly longer than sham-treated groups (median survivals 31.5 or 40 days) and exhibited good safety/toxicity profiles.

**Conclusion**—The results indicate combining cellular and suicide gene therapies is a viable strategy for the treatment of established breast tumors in the brain.

### Keywords

breast cancer; brain cancer; metastasis; gene therapy; immunotherapy

## INTRODUCTION

Breast cancer is the most common malignancy in women in the United States and metastasis is a major cause of morbidity and mortality in these patients. With improvements in the control of visceral and bone metastasis, the incidence of brain metastasis is rising (1–3). The progressive neurological disabilities associated with brain metastasis not only impair the quality of life but also decrease the survival. The biology of the brain and blood brain barrier, and the fact that brain metastases can present as multiple lesions often characterized by nests of infiltrating tumor cells surrounding the larger brain metastases (4, 5) make the management of brain metastases very challenging. Currently therapeutic approaches include whole brain radiation therapy and stereotactic radiosurgery usually administered as palliative care (6–8).

Newer approaches include the use of tumor-targeted cytotoxic T lymphocytes for adoptive immunotherapy. A unique form of adoptive T cell therapy for brain tumors involves the use of alloreactive cytotoxic T lymphocytes (alloCTL), potent cytotoxic T cell effectors that are trained to recognize non- or aberrant-self class I and II human leukocyte antigens (HLA). They are generated by sensitization of peripheral blood mononuclear cells (PBMC), isolated from a healthy donor, to the HLA of the tumor-bearing host (9–11). The HLA primarily acts as tumor-directed antigen in the brain, since its expression, especially Class I, is absent on normal neuroglia, i.e., neurons, oligodendrocytes, and astrocytes (12–14), but is highly expressed on brain tumor cells (13, 15–18).

Another new therapeutic approach is the use of replicating virus vectors for gene therapy or oncolytic virotherapy. Recently, it has been demonstrated that replicating retroviral vectors (RRV), unlike their replication-defective counterparts, exhibit sustained transduction in dividing cancer cells and can efficiently transfer transgenes throughout solid tumors (19–24). Glioma-bearing rats demonstrate significantly prolonged survival when given RRV coding for the prodrug activator gene, yeast cytosine deaminase (CD) followed by multiple administrations of 5-fluorocytosine (5-FC) prodrug (20–22). The lack of detectable spread of the RRV to normal tissues additionally provides an element of safety in this approach (21, 23, 25).

Both alloCTL adoptive immunotherapy and RRV-mediated prodrug activator gene therapy have been studied individually in patients with primary brain tumors. Notably, the clinical feasibility and safety of intratumoral alloCTL treatment was initially tested in a small pilot study (9, 11), in which three recurrent Grade III glioma patients receiving this treatment exhibited survival longer than expected. These data led to the initiation of a Phase I dose-escalation study at UCLA, now accruing patients ([www.clinicaltrials.gov](http://www.clinicaltrials.gov), NCT01144247). As well, RRV encoding CD for prodrug activator gene therapy has advanced to the clinic for recurrent high-grade gliomas ([www.clinicaltrials.gov](http://www.clinicaltrials.gov), NCT 01156584 and NCT 0147094).

Clinically, brain metastases are more common than primary brain tumors (26), and represent a dire clinical situation in need of effective therapies. Here, we evaluated both of these

cellular and gene therapy approaches, individually and in combination, for the treatment of intracranial breast tumors. Our results demonstrate that alloCTL generated to the breast tumor cell line MDA-MB-231 (231) showed cytotoxicity, proliferation, and interferon-gamma (IFN $\gamma$ ) production in response to coincubation with the parental target cell line, as well as with two metastatic sublines (27, 28). Intracranially placed alloCTL were capable of migrating from one established intracranial tumor focus to another in contralateral brain over a relatively short time span (6 hr) in immune-incompetent mice, and apoptotic tumor cells were observed in proximity to these CTL. Using subcutaneous and intracranial human breast tumor xenograft models, we found that combining prodrug activating gene therapy with alloCTL adoptive transfer resulted in improved outcome compared to the benefit seen with each therapy individually. Our findings thus support clinical translation of this multi-modal approach.

## MATERIALS AND METHODS

### Cell lines and HLA expression

The human breast tumor cell line MDA-MB-231 (231; ATCC, Manassas, VA) was grown in L15 medium supplemented with 10% fetal bovine serum (FBS; Aleken, Nash, TN). The brain-seeking 231 subline, 231BR (27), the bone-seeking 231 subline, 231-1833 (28), and 293T human embryonic kidney cells (ATCC) were maintained in Dulbecco's modified Eagles medium (DMEM) supplemented with 10% FBS, sodium pyruvate and penicillin/streptomycin (Sigma, St. Louis, MO). Class I HLA display was determined on breast cancer cell lines by flow cytometric analysis using RPE-conjugated mouse anti-human HLA-ABC antibody and a mouse RPE-conjugated IgG served as isotype control (eBiosciences, San Diego, CA). The percentage of positive cells and relative antigen density indicated by mean fluorescence intensity (MFI) were determined (13). Specific HLA-ABC types were determined by low resolution molecular HLA typing (University of California, San Diego, Torrey Pines Clinical Laboratory, San Diego, CA).

### Generation of alloCTL enriched cultures by one-way mixed lymphocyte tumor reaction (MLTR)

PBMC were isolated from leukopaks of healthy donors undergoing leukapheresis (UCLA Institutional Review Board approved protocol) using density gradient centrifugation as previously described (10). Prior to one-way MLTR, 231 cells underwent 48-hr incubation in culture medium with 500 IU/ml recombinant human IFN $\gamma$  (RD Systems Inc., Minneapolis, MN) to upregulate their HLA expression (13). The stimulator (S) 231 cell monolayers were then washed with phosphate buffered saline (PBS) and detached with 2 mM EDTA containing 1% BSA, washed and inactivated with 7000 rad (X-ray Irradiator, Gulmay Medical, Inc., Atlanta, GA). Responder (R) PBMC were mixed with inactivated S cells at a R:S ratio of 10:1. The cell mixtures were placed into Aim-V medium (Life Technologies, Inc., Grand Island, NY) containing 5% heat-inactivated autologous plasma and 60 International Units (IU) of recombinant human interleukin-2 (IL-2)/ml (Proleukin, Novartis, San Carlos, CA). Growth was monitored daily and cultures were fed and maintained as previously described (10). AlloCTL preparations were used in assays between 12 to 14 days post-MLTR.

### Plasmid constructs and viral vector production

The pAC3-yCD2 and pAC3-GFP plasmid constructs, encoding amphotropic Moloney murine leukemia virus (MuLV) carrying expression cassettes consisting of an internal ribosome entry site (IRES) followed by either CD or green fluorescent protein (GFP) transgenes, respectively, have been described previously (23, 24).

Viral vector stocks were generated by transfection of 293T cells using the FuGENE6 transfection agent (Roche Molecular Biochemicals, Mannheim, Germany) per manufacturer instructions (22). Conditioned medium (viral supernatant) was collected 48 hr after transfection with either the pAC3-GFP or pAC3- $\gamma$ CD2 plasmids (23, 24).

Concentrated viral vector supernates were prepared from 293T stable vector producing cells. Conditioned medium was harvested after 72-hr incubation, and clarified by centrifugation before 100-fold volume concentration using a Vivaspin-20 (Sartorius Stedim, Gottingen, Germany) per manufacturer protocol. Control supernatant from nontransduced, non-vector producing 293T cells was harvested and concentrated in parallel. Concentrated viral titers were approximately  $10^6$  transducing units/ml when tested using either 293T or 231BR cells. The titer was determined 48 hr after adding 50  $\mu$ M of 3'-azido-deoxythymidine (AZT, Sigma Aldrich, St. Louis, MO) to the cultured cells to prevent further virus replication as described (20, 29). For subcutaneous (sc) tumors, 10  $\mu$ l of concentrated vector producing or non-vector producing supernatants were admixed with tumor cells immediately before injection.

### Anti-tumor functionality assessments of alloCTL

**Cytotoxicity Assay**—Lytic activity of alloCTL was assessed at various effector to target ratios (E:T) by  $^{51}\text{Cr}$  release cytotoxicity assays at 12–14 days post-MLTR (9). Target cells were labeled with 100  $\mu$ Ci  $\text{Na}_2^{51}\text{CrO}_4$  (Amersham, Park Ridge, IL) and the assay was performed as previously described (Hickey, 2012 #249). Maximal release was obtained from targets incubated with 0.1 M HCl, and spontaneous release was the radioactivity released from targets in assay medium alone. The percentage specific release was calculated by the formula:  $[(^{51}\text{Cr}_{\text{experimental}} - ^{51}\text{Cr}_{\text{spontaneous}}) / (51\text{Cr}_{\text{maximal}} - ^{51}\text{Cr}_{\text{spontaneous}})] \times 100\%$ . Mean specific release  $\pm$  standard error of the mean (SEM) was determined from triplicate wells.

**Cytokine Production**—Human IFN $\gamma$  concentrations were measured in clarified supernates collected 48 hr after coincubation of day 12 alloCTL with relevant tumor target cells. Aliquots of the alloCTL from the same preparation either were or were not restimulated at day 12 post-MLTR with 231 or sublines, 231-1833 or 231BR, at a R:S of 10:1. Manufacturer instructions were followed for a Quantikine ELISA kit specific for human IFN $\gamma$  (R&D Systems, Minneapolis, MN) with a sensitivity of 2 pg/ml (30).

**Immunophenotype and proliferation of restimulated alloCTL**—At 12 days post-MLTR alloCTL were restimulated with 231 cells or sublines for 72 hr at a R:S ratio of 10:1 in culture medium containing bromodeoxyuridine (BrdU, BD Biosciences, San Jose, CA). GolgiStop (BD Biosciences) was added to block protein transport during the last 5 hr of culture. Cells were washed and surface-stained with APC-conjugated anti-CD4, PeCy5-conjugated anti-CD8 for 15 min at 4 $^{\circ}$ C, washed again, fixed and permeabilized according to instructions for the BD BrdU Flow Kit (BD Biosciences, San Diego, CA). Cells were then intracellularly stained with PE-conjugated anti-IFN $\gamma$  and FITC-conjugated anti-BrdU for 30 min at 4 $^{\circ}$ C, washed, resuspended and immunophenotyped using a BD LSRII flow cytometer running BD-DIVA acquisition software. Dot blots were analyzed using FlowJo flow cytometric analytic software.

### *In vivo* studies with human 231BR xenografts

Rag2 $^{-/-}$  $\gamma$ c $^{-/-}$  mice were purchased from Taconic Farms (Hudson, NY) (31). All animal experiments were performed according to institutional guidelines under approved protocols.

**Subcutaneous tumor model**—231BR cells ( $2 \times 10^6$ ) were coinjected with concentrated RRV-GFP, RRV-CD, or concentrated non-viral control supernate sc in the right flank of 6-week old mice. After allowing tumors to establish for 15 days, mice were randomized to treatment groups ( $n=4-6$ ). Certain groups were treated with intratumoral alloCTL ( $1.2 \times 10^7$ ). All mice were treated with 5-FC (500mg/kg) intraperitoneally (ip) every day from days 21–27. Caliper measurements of tumor width and length were performed every 3–4 days. Tumor volumes were calculated for individual animals using the formula: Volume =  $(4/3)\pi(\text{width}/2)^2(\text{length}/2)$  (32). Mean tumor volumes for each treatment group  $\pm$  SEM were plotted over time.

**Intracranial vector spread**—100% RRV-GFP transduced 231BR (231BR-GFP) cells were admixed with nontransduced 231BR at 2% or 8% of the total tumor cell inoculum ( $2 \times 10^5/3 \mu\text{l}$ ). Cells were then placed into the right side of the brain through a burr hole, 2 mm lateral and 1mm anterior to the bregma, at a depth of 3 mm. Groups of mice ( $n=3$ ) were sacrificed on days 7, 14, and 20 post-tumor instillation, and brains were harvested. Tumor tissue at the injection site was excised (approximately  $5 \times 5 \times 5 \text{ mm}^3$ ), minced and digested in collagenase/dispase (1mg/ml; Roche, USA) as described (22). Single cell suspensions were stained with fluorescent APC anti-HLA-ABC (eBiosciences, San Diego, CA) and flow cytometrically analyzed.

**Intracranial alloCTL motility studies**—231BR cells ( $2 \times 10^5$  each) were stereotactically injected into the above coordinates and its enantiomeric position, such that right and left hemispheric tumor foci could develop. Tumors were allowed to establish 18 or 21 days before alloCTL ( $2 \times 10^6$ ) were injected into the left tumor foci. Mice were sacrificed 6 hr later, and brains were harvested, placed into 10% buffered formalin, paraffin-embedded, sectioned, and diaminobenzidine immunostained using rabbit anti-human CD3 (Clone SP7, Genway Biotech Inc., San Diego, CA) with hematoxylin counterstain and evaluated by light microscopy.

**Intracranial efficacy studies**—Mice underwent surgery for placement of intracranial cannulas (Plastics One, Roanoke, VA) that were placed through a burr hole in the right side of the skull at the above coordinates. The cannulas extended 3 mm into the brain and affixed to the skull with resin. Six days later, tumor cells ( $2 \times 10^5$  total cells in  $3 \mu\text{l}$ ), consisting of either 100% 231BR, or 98% 231BR cells + 2% 231BR-GFP or 2% 231BR-CD cells, were infused through the cannulas into various treatment groups. AlloCTL or unstimulated PBMC ( $2 \times 10^6/3 \mu\text{l}$ ) or PBS were infused through the cannulas into the tumor on days 9 and 16 post-tumor instillation. All groups of mice ( $n=9-10$ ) were treated with 3 cycles of 5 daily ip 5-FC (500 mg/kg) injections (per cycle) beginning on days 12, 26 and 47 post-tumor instillation. Mice were monitored for signs of morbidity and weighed every 3–4 days for the duration of the experiment.

### Analysis of RRV biodistribution

To harvest brains, coronal cuts were made at the site of cannula implantation and 4 mm posterior to that cut. The anterior sections were snap-frozen for quantitative real time polymerase chain reaction (qRT-PCR) to determine RRV biodistribution; the posterior 4 mm sections were fixed in formalin, paraffin-embedded and the blocks were sectioned ( $5 \mu\text{m}$ ) before staining with hematoxylin and eosin (H&E).

Genomic DNA was extracted using the DNeasy tissue kit (Qiagen, Valencia, CA) from tissues (liver, spleen, kidney, bone marrow, and brain) of all long-term survivors and representative animals derived from control and experimental groups that succumbed to tumor after intracranial treatment with RRV and/or alloCTL. To detect integrated RRV

sequences, qRT-PCR amplification of genomic DNA was carried out in duplicate with TaqMan Universal PCR Master Mix (PE Applied Biosystems, Foster City, CA) using a My-iQ2 Biorad Thermal Cycler. The primers and probe were designed to target the 4070A amphotropic env gene (4070A-F, 5'-GCGGACCCGGACTTTTGA-3'; 4070A-R, 5'-ACCCCGACTTTACGGTATGC-3'; probe, FAM-CAGGGCACACGTAAAA-NFQ). Human RNase P (hRNase P) and mouse  $\beta$ -actin (m $\beta$ -actin) were also quantified as reference genes using TaqMan RNase P Detection Reagents and Custom TaqMan Gene Expression Assays (Applied Biosystems), which is designed to target mouse  $\beta$ -actin gene ( $\beta$ -actin-forward, 5'-GGTCGTACCACAGGCATTGT-3';  $\beta$ -actin-reverse, 5'-CTCGTAGATGGGCACAGTGT-3'; probe, FAM-CCCGTCTCCGGAGTCC-NFQ). A standard curve for copy number was prepared by amplifying serial dilutions of plasmid pAC3-yCD2 in a background of genomic DNA from nontransduced cells.

### Statistical analyses

GraphPad Prism software (version 4, GraphPad Software, San Diego, CA) was used to analyze the *in vitro* and *in vivo* data. The Student t-test determined significance differences between the percentage lysis of target tumor cells with and without the addition of anti-HLA; *p*-values  $\leq 0.05$  were significant. Experimental and control groups for the *in vitro* restimulation experiments measuring proliferation, immunophenotype and cytokine production, and the *in vivo* subcutaneous tumor volume comparisons at given times were compared using a 2-way ANOVA with Bonferroni correction and *p*-values  $\leq 0.05$  divided by the number of comparisons (3) in experiments described in Figures 2 and 4 were considered significant. Mean survival times (MST) from the Kaplan Meier curves were analyzed by nonparametric Log-Rank tests.

## RESULTS AND DISCUSSION

### HLA Class I on breast tumor cells and upregulation with IFN $\gamma$

Flow cytometric analysis showed that nearly all (94–99%) of the cells in the parental 231 line, as well as 231-1833 and 231BR sublines, expressed HLA Class I and their incubation with IFN $\gamma$  resulted in 1.4–1.5 fold increases in MFI (Supplemental Table 1). HLA-ABC expression after IFN $\gamma$  induction was highest on the parental 231 cell line (MFI 1402 + 49.7) compared with slightly lower expression by each of the sublines, thus making the parental 231 cells most desirable as stimulator cells in a one-way MLTR for alloCTL generation. The low resolution molecular type of HLA-ABC loci in 231 cells was HLA-A\*02, B\*41,\*40, and C\*17,\*02 (Supplemental Table 2).

### AlloCTL exhibit anti-tumor function *in vitro*

The standard method for generating alloCTL is by one-way mixed lymphocyte reaction (MLR) where inactivated stimulator PBMC from the cancer patient are combined with responder PBMC from healthy donors genetically-distinct from the patient (10). However, because PBMC are not available from the patient from whom 231 breast tumor cells were derived, to generate alloCTL we used a one-way MLTR where 231 tumor cells were incubated with IFN $\gamma$  to upregulate HLA Class I expression as above, then inactivated and used as stimulator cells with responder PBMC isolated from HLA-mismatched allogeneic donors (33).

Four different donors provided PBMC that served as sources of precursor alloCTL for these experiments. All donors were mismatched at 4–5 class I HLA-ABC alleles compared to that displayed by the 231 stimulator cells (Supplemental Data Table 2). The HLA types of alloCTL used for *in vitro* and *in vivo* experiments are provided and associated with data in particular Figures. Note these preparations will contain CTL directed to minor tumor

associated antigens as well as HLA, albeit the precursor frequency for CTL within PBMC would be higher to major than to minor antigens (34–36).

To determine if the alloCTL made by MLTR had anti-tumor function *in vitro* we performed cytotoxicity assays on day 14 following one-way MLTR. AlloCTL effector cells were mixed with <sup>51</sup>Cr-loaded 231, 231-1833 or 231BR target cells at a range of E:T ratios for 4 hr. As expected, and in a dose-dependent manner, the ability of alloCTL to kill each of the three target cell lines was similar; there were no significant differences in the percentages of lysis obtained at each E:T ratio (Figure 1). Furthermore, the cytolysis induced by alloCTL to 231 and its sublines is in part HLA-restricted, as indicated by significant inhibition of cytotoxicity (33.3–41.3% reduction in percentage lysis of 231 and variants,  $p < 0.006$ ) upon antibody-mediated blockade of HLA. We replicated the cytotoxicity findings with alloCTL (with and without blocking antibody to HLA) using two other breast cancer cell lines, BMC Brain2 and MDA-MB-361 (unpublished data).

### alloCTL subset proliferation and IFN $\gamma$ production following restimulation

The ability of the CD4<sup>+</sup> and CD8<sup>+</sup> T cell subsets within the alloCTL preparations to proliferate and produce IFN $\gamma$  following restimulation with 231, 231-1833, or 231BR target cells was evaluated. AlloCTL that had been restimulated on day 12 post one-way MLTR for 72 hr at a 10:1 R:S ratio with one of the three relevant cell lines, or left unstimulated, were surface-stained for CD4 and CD8, and then fixed, permeabilized and stained for proliferation marker (BrdU) and proinflammatory IFN $\gamma$  production. Figure 2 shows data obtained from a representative alloCTL preparation. The percentages of CD8<sup>+</sup> T cells that incorporated BrdU upon restimulation and thus proliferated upon stimulation with relevant target cells were significantly higher ( $p < 0.017$ ) compared to those that were unstimulated (Figure 2A). Lymphocyte proliferation occurred equally well with parental 231 cells and the metastatic sublines, 231-1833 or 231BR. In contrast, there were no significant differences in BrdU incorporation between CD4<sup>+</sup> T cells that were restimulated versus those that were unstimulated (Figure 2A), indicating lack of CD4<sup>+</sup> subset proliferation, regardless of whether restimulation was performed with the parental 231 cells or the 231-1833 or 231BR subline counterparts.

The total percentages of CD8<sup>+</sup> T cells were significantly higher ( $p < 0.017$ ) within alloCTL populations that were restimulated with relevant target cells (51.8–56%) compared to unstimulated alloCTL (30.9%) (Figure 2B). Because the CD8<sup>+</sup> cells proliferated when restimulated with 231, 231-1833, and 231BR cells and the CD4<sup>+</sup> cells did not, the total percentages of CD4<sup>+</sup> T cells were significantly reduced ( $p = 0.017$ ) compared to the unstimulated counterpart (Figure 2C). The data show that restimulation of alloCTL with 231, 231-1833, or 231BR breast cancer cells results in a significant shift in T cell subsets that make up the alloCTL culture.

Expression of IFN $\gamma$  following 72 hour restimulation with 231, 231-1833, and 231BR, compared to unstimulated cells, was also evaluated. Protein transport was blocked during the last 5 hr of culture to allow intracellular accumulation of IFN $\gamma$ . Expression of IFN $\gamma$  was significantly higher ( $p = 0.017$ ) within CD8<sup>+</sup> T cells that were restimulated with 231, 231-1833, or 231BR, compared to cells that were unstimulated (64.6, 45.1, 43.8 vs. 27.5, respectively; Figure 2D). Production was more robust when restimulation was performed with the parental cells versus the sublines, correlating with the relative antigen densities (MFIs) of cell-surface Class I HLA (Suppl Table 1), suggesting that this parameter may have some influence over response. In contrast, production of IFN $\gamma$  in CD4<sup>+</sup> T cells was not affected following restimulation with any of the cell lines (data not shown).



To confirm the above observations, IFN $\gamma$  secretion by alloCTL at day 12 post-MLTR was analyzed from supernates collected 48 hr following restimulation with relevant target cells, and compared with IFN $\gamma$  secreted by unstimulated alloCTL. The average secretion of IFN $\gamma$  by restimulated alloCTL cocultured with 231, 231-1833 and 231BR ( $17.2 \pm 1.2$ ,  $16.9 \pm 0.50$ , and  $13.2 \pm 0.97$  ng/ml, respectively) was significantly elevated ( $p < 0.017$ ) compared to that of unstimulated alloCTL ( $7.4 \pm 0.21$  ng/ml).

### **alloCTL migrate through and to distant tumor foci *in vivo* and induce apoptosis**

We examined the migratory capacity of alloCTL in the context of multifocal intracranial tumors. As shown in Figure 3A, bilateral 231BR tumors were established intracranially in the right and left hemispheres of Rag2 $^{-/-}$  $\gamma$ c $^{-/-}$  mice, and allowed to grow for 21 days. AlloCTL specific for 231 HLA were then stereotactically injected into the tumor bed on the right side (Figure 3A), and coronal sections of brain were prepared 6 hr later and immunostained with a human CD3-specific antibody (Figures 3B–G). Figure 3B shows a representative low power photomicrograph of a coronal brain section with bilateral tumor foci. Intermediate power magnification of the tumor (Figure 3C) in the right side of the brain shows numerous DAB-stained (rust-color) human CD3+ T lymphocytes (black arrows) penetrating the tumor mass at the instillation site. A higher power magnification photomicrograph (Figure 3D) from the same area shows CD3+ cells (black arrows) in proximity to a necrotic tumor cell with a fragmented nucleus indicating cell death (white arrows). Additionally, CD3+ alloCTL have trafficked and localized to established tumor in contralateral brain (Figures 3E–G). Rust colored CD3+ cells are shown having permeated the tumor mass (t) on the left side and also appear in perivascular spaces (asterisks), which is a path for tumor invasion (Figure 3E), while no CD3+ cells are visible in normal brain. Intermediate and higher power magnification photomicrographs (Figures 3F–G) similarly demonstrate larger, activated CD3+ T cell phenotypes (black arrows) in close juxtaposition to apoptotic tumor cells (white arrows), indicating cytotoxic functionality may be retained by the trafficking alloCTL.

### **Cellular and gene therapies demonstrate therapeutic benefit in subcutaneous 231BR xenograft models**

To determine if cellular and gene therapy approaches individually or in combination would be efficacious *in vivo*, Rag2 $^{-/-}$  $\gamma$ c $^{-/-}$  mice were injected subcutaneously with 231BR (initial inoculum  $2 \times 10^6$  cells) admixed with RRV-GFP, RRV-CD or control non-viral supernatant. Tumors were allowed to establish for 15 days before some experimental groups were treated with intratumoral alloCTL ( $1.2 \times 10^7$  cells). All groups ( $n=4-6$ ) received the suicide gene therapy prodrug, 5-FC (500 mg/kg ip) on days 21–27. Tumor volumes monitored over time showed significant differences between the control and experimental groups starting from day 25 ( $p < 0.017$ ; Figure 4). The two control groups that received 231BR with non-therapeutic RRV-GFP or control non-viral naïve 293 cell supernatant at the start of the experiment both exhibited progressive tumor growth *in vivo*, with average group tumor volumes at day 28 of  $759 + 243$  mm $^3$  and  $659 + 114$  mm $^3$ , respectively. Therapeutic benefit was noted for all experimental treatment groups (groups that received RRV-CD, alloCTL or a combination of the two) compared to mice that received tumor with concentrated non-viral supernatant. Tumors treated with RRV-CD alone, without alloCTL injection, showed significant ( $p = 0.017$ ) tumor growth inhibition upon application of 5-FC prodrug treatment between days 25 to 27 compared to control groups. Tumors treated with non-viral supernatant but receiving intratumoral alloCTL also showed significant ( $p = 0.017$ ) tumor growth inhibition compared to control groups, following cellular therapy, but as expected, did not show response to prodrug administration. Notably, the greatest reduction in mean tumor volumes was obtained when intratumoral cellular therapy with alloCTL was combined with prodrug activator gene therapy with RRV-CD/5-FC ( $p = 0.017$ ). We obtained

similarly efficacious findings in a second tumor model employing subcutaneous U-87MG glioma xenografts (Haga K et al., manuscript in preparation). In those experiments, a more clinically-relevant scenario was tested where tumors were allowed to establish for one-week before infusing with RRV-CD supernatant and/or alloCTL. This experimental paradigm required an *in situ* transduction of pre-established tumor to obtain a beneficial effect from administered prodrug. Again, efficacy was observed for the individual as well as the combination therapies.

### **RRV effectively spreads through intracranial breast tumor xenografts**

RRV can achieve significantly enhanced transduction compared to their replication defective counterparts (19). RRV exhibit an amplification process that is inherent to the wild type virus life cycle, so while viral replication kinetics and lag times for exponential growth phase replication can vary, even a slower replication will allow progressive vector spread within a tumor until prodrug is given. We have previously demonstrated RRV replication and gene expression in subcutaneous mammary tumors (29). To evaluate RRV spread in intracranial breast tumors, Rag2<sup>-/-</sup>γc<sup>-/-</sup> mice were intracranially injected with  $2 \times 10^5$  naïve 231BR cells mixed supplemented with either 2% or 8% RRV-GFP transduced 231BR cells (231BR-GFP). Transduction of the tumor by RRV was evaluated by flow cytometry on days 7, 14 and 20 post-tumor instillation (Figure 5A and B). To distinguish the human 231BR tumor cells from mouse brain cells, enzyme-digested tumor tissues were stained with fluorescently labeled human-specific anti-HLA-ABC and the percentages of GFP+ cells within this population were quantified. When the initial tumor inoculum contained either 2% or 8% 231BR-GFP cells, by day 7 post-tumor instillation approximately 57% of the human Class I HLA-ABC+ tumor cells had been transduced with RRV-GFP. Subsequently, tumor transduction levels rose to ~75–83% at 20 days following tumor instillation. Figure 5B shows representative flow cytometric dot-plots from day 14, indicating 71.2 + 3.7% and 78.9 + 1.1% GFP transduction of HLA-ABC+ human 231BR cells after initial tumor inoculation with 2% and 8% 231BR-GFP cells, respectively.

### **Individual and combined cellular (alloCTL) and gene (CD) therapies are safe and exhibit therapeutic benefit in intracranial 231BR xenograft models**

The efficacy of combined cellular alloCTL immunotherapy with RRV prodrug activator gene therapy was tested in Rag2<sup>-/-</sup>γc<sup>-/-</sup> mice bearing established intracranial 231BR tumors. Indwelling intracranial cannulas were used to establish intracerebral tumors in 7 groups (n=9–10) of mice, consisting of either 100% 231BR, or 98% 231BR mixed with either 2% 231BR-GFP or 2% 231BR-CD cells (Figure 6). Control groups of mice were injected with non-therapeutic 231BR-GFP tumor cells instead of 231BR-CD, or were infused with PBS or unstimulated PBMC in place of alloCTL. On days 9 and 16 post-tumor instillation, effector alloCTL, or control PBMC or PBS was infused into the established tumor bed through the cannula. All mice were treated with 5-day cycles of 5-FC (500mg/kg, ip); up to 3 cycles were possible, spaced 2 or 3 weeks apart beginning on day 12 post tumor instillation (Figure 6A). Kaplan Meier survival plots and MST for the control and experimental groups are shown in Figure 6B. The MST of the untreated control group (no RRV, no alloCTL effector cells, group 1) was 31.5 days, while the MST of the sham-treated control group given non-therapeutic 231BR-GFP vector producing cells with the tumor inoculum and unstimulated PBMC was 40 days (group 3). The MSTs for mice treated with individual experimental modalities ranged from 50 to 83 days. The MSTs of the two groups receiving alloCTL therapy alone (with RRV-GFP infection, or no RRV infection) were 65 and 83 days respectively (groups 4 and 2), while the MSTs of the two groups receiving prodrug activator gene therapy alone (with PBMC or PBS, instead of alloCTL) and up to 3 prodrug cycles were 50 and 57 days, respectively (groups 6 and 5). Statistical significance was reached ( $p < 0.05$ ) for all of the individual immune or gene therapy treated groups

compared to each of the control groups (Figure 6C). The MST of the group receiving the *combined* intratumoral effector alloCTL and RRV prodrug activator gene therapies (group 7) was 97.5 days, thus exhibiting a highly statistically significant survival benefit compared to each of the control groups (Figure 6C). Furthermore, the group receiving combined immune and gene therapies showed a statistically significant additional survival advantage compared to those groups receiving gene therapy alone ( $p < 0.0001$  and  $0.0123$ , groups 7 vs. 6 and 5, respectively). The combination treatment also showed a trend toward statistical significance compared to the groups receiving alloCTL cellular therapy alone ( $p < 0.0511$  and  $0.6380$ , groups 7 vs. 4 and 2, respectively).

The individual animal weights of Figure 6 animals were monitored every 3–4 days and plotted over the duration of the experiment as one indication of treatment toxicity and/or morbidity due to tumor progression. The plots for the control groups, and the single or combined modality groups are shown starting on day 12 through 106 with prodrug cycle administration indicated on the abscissa (Supplemental Figure 1). The plots not only show the extension of survival of animals in the experimental groups, but as well, indicate the health of the 11 long-term survivors present in groups 2, 4, 5, and 7. Except in sham-treated control animals (Groups 1 and 3), generally little to no weight loss occurred during or shortly after the first prodrug cycle and second alloCTL infusion. Progressive weight loss at later time points was likely associated with higher tumor burden, and notably, stabilization or reversal of weight loss was observed following prodrug administration cycles in individual animals in Groups 2, 5, 6, and 7; this was most apparent after the last prodrug cycle in Groups 2 and 7, and most of those animals went on to thrive as indicated by stable or increasing weight gains. Thus, treatment with intracranial infusions of alloCTL as well as prodrug administration in RRV-CD treated animals both contributed positively to overall clinical response to therapy as measured by average body weight, and mice treated with combined immunogene therapy had the highest overall average weight throughout the course of treatment.

Histopathological findings of the brains from the long-term survivors ( $n=11$ , from Figure 6 experimental Groups 2, 4, 5 and 7) showed no evidence of tumor in H&E-stained sections, whereas there was consistent presence of tumor in animals that succumbed before the end of the survival experiment (Supplemental Figure 2).

To monitor the spread of RRV-GFP or RRV-CD within the brain and to extratumoral sites, genomic DNA was extracted from brain/brain tumor, lung, liver, spleen, kidney, and bone marrow tissues, then analyzed by qRT-PCR using primers and probe sequences specific for the 4070A amphotropic envelope. Data are shown as RRV copy number/ $5 \times 10^4$  cells and calculated as detailed in Supplemental Table 3. In the long-term survivors from the experimental treatment groups (Figure 6), there were low or no detectable levels of RRV signals, which correlated with the apparent absence of tumor by histopathology. In tumor-bearing animals, there were also higher levels of virus; representative data are shown for one animal in group 7 that succumbed to tumor on day 90. As expected in immunodeficient animal models, RRV signals indicating extratumoral vector spread were largely restricted to hematopoietic tissues, and in other tissues, the lymphoid cell content within them (37).

Overall, our results demonstrate proof-of-concept that a unique combination regimen, consisting of cellular therapy with alloCTL and gene therapy employing RRV encoding a prodrug activator gene, represents a promising strategy to treat breast tumors metastatic to the brain. We postulate that the mechanisms at work benefiting the combined treatment might involve alloCTL favorably improving the dissemination of RRV to metastatic foci. This could either be by 1) adsorption of virus particles to the surface of trafficking T cells that then transduce tumor cells, i.e., a “hitch-hiking” mechanism without involving actual

infection of T cells (38), or 2) a small percentage of alloCTL that become transduced and then act as motile vector producing cells to carry the vector to other tumor foci. Suicide gene therapy may also augment the immediate effects of adoptive cellular therapy, since tumor cell injury (combined apoptosis + lysis) induced by effector T cells or suicide gene therapy could improve endogenous immune function by presentation of fragmented tumor cells and antigens to T cells. It is possible that further therapeutic gains can be realized, particularly in immunodeficient xenograft models, by administering additional cycles of prodrug, as previously reported (20), and by adjusting the timing and sequencing of alloCTL infusion vs. prodrug administration. Although the xenograft model used in these studies did not allow a determination of the degree of inflammation induced by the viral vector interacting with endogenous immune cells in the brain, prior studies in a syngeneic animal model indicate that this is not a problem (21). In fact, recent studies in syngeneic intracranial glioma models show that an intact endogenous immune system can contribute to complete tumor eradication after RRV-mediated prodrug activator gene therapy, as well as to restriction of systemic viral spread to normal tissues (23). Activation of endogenous anti-tumoral immune responses due to destruction of the immunosuppressive tumor environment and release of immunostimulatory cytokines from adoptively transferred alloCTL may also contribute to further therapeutic benefit. As alloCTL and RRV therapies have now individually reached the clinical testing stage, we can envision the clinical design for combination immunogene therapy of breast cancer metastatic to brain to be feasible, as shown in Supplemental Figure 3. In summary, continued preclinical and clinical investigation of combined, local cellular and gene therapy regimens are warranted for brain metastases.

## Supplementary Material

Refer to Web version on PubMed Central for supplementary material.

## Acknowledgments

The MDA-MB-231BR and MDA-MB-231-1833 human breast cancer cell lines were kindly provided by Drs. T. Yoneda (University of Texas Health Science Center, San Antonio, TX) and J. Massague (Memorial Sloan Kettering Cancer Center, NY, NY), respectively.

### GRANT SUPPORT

Financial support for the study was supplied in part by USAMRMC W81XWH-08-1-0734 (CAK), CBCRP 14IB-0114A (BMM), NIH RO1 CA121258 (NK), NIH/NCATS UCLA CTSI Grant Number UL1TR000124 (CAK/NK), the Joan S. Holmes Memorial Research Fund (CAK), the Joan S. Holmes Memorial Postdoctoral Fellowship (MJH), and an unrestricted gift donation from Tocagen, Inc. to the Regents of the University of California. YK is the recipient of a predoctoral fellowship from the Japan Student Services Organization. AI is the recipient of a postdoctoral fellowship from the Susan G. Komen Breast Cancer Foundation.

## Abbreviations

<b>5-FC</b>	5-fluorocytosine
<b>alloCTL</b>	alloreactive cytotoxic T lymphocytes
<b>alloCTL/RRV</b>	alloCTL preparations transduced with RRV
<b>BrdU</b>	bromo-deoxyuridine
<b>CD</b>	cytosine deaminase
<b>CTL</b>	cytotoxic T lymphocyte
<b>DAB</b>	diaminobenzidine

<b>DMEM</b>	Dulbecco's modified Eagles medium
<b>E:T</b>	effector to target
<b>FBS</b>	fetal bovine serum
<b>GFP</b>	green fluorescent protein
<b>HBSS</b>	Hank's balanced salt solution
<b>H&amp;E</b>	hematoxylin and eosin
<b>HLA</b>	human leukocyte antigens
<b>IFN<math>\gamma</math></b>	interferon-gamma
<b>IL-2</b>	interleukin-2
<b>IU</b>	international units
<b>ic</b>	intracranial
<b>ip</b>	intraoperative
<b>231</b>	MDA-MB-231 cells
<b>231BR</b>	231 variant brain tropic subline
<b>231-1833</b>	231 variant bone and brain tropic 231 cells
<b>MFI</b>	mean fluorescence intensity
<b>MST</b>	median survival time
<b>MLR</b>	mixed lymphocyte reaction
<b>MLTR</b>	mixed lymphocyte tumor reaction
<b>PBMC</b>	peripheral blood mononuclear cells
<b>PBS</b>	phosphate buffered saline
<b>RRV</b>	retroviral replicating vector
<b>R</b>	responder
<b>R:S</b>	responder to stimulator ratio
<b>SEM</b>	standard error of the mean
<b>S</b>	stimulator
<b>TU</b>	transducing units
<b>VPC</b>	vector producing cells

## References

1. Sharma M, Abraham J. CNS metastasis in primary breast cancer. *Expert Rev Anticancer Ther.* 2007; 7:1561–6. [PubMed: 18020924]
2. Cheng X, Hung MC. Breast cancer brain metastases. *Cancer Metastasis Rev.* 2007; 26:635–43. [PubMed: 17717635]
3. Seidman AD. Brain metastases from breast cancer. *Clin Adv Hematol Oncol.* 2010; 8:595–7. [PubMed: 21157408]
4. Palmieri D, Bronder JL, Herring JM, Yoneda T, Weil RJ, Stark AM, et al. Her-2 overexpression increases the metastatic outgrowth of breast cancer cells in the brain. *Cancer Res.* 2007; 67:4190–8. [PubMed: 17483330]

5. Palmieri D, Chambers AF, Felding-Habermann B, Huang S, Steeg PS. The biology of metastasis to a sanctuary site. *Clin Cancer Res.* 2007; 13:1656–62. [PubMed: 17363518]
6. Eichler AF, Loeffler JS. Multidisciplinary management of brain metastases. *Oncologist.* 2007; 12:884–98. [PubMed: 17673619]
7. Hemphill MB, Lawrence JA. Current therapeutic options for breast cancer central nervous system metastases. *Curr Treat Options Oncol.* 2008; 9:41–50. [PubMed: 18392684]
8. Platta CS, Khuntia D, Mehta MP, Suh JH. Current treatment strategies for brain metastasis and complications from therapeutic techniques: a review of current literature. *Am J Clin Oncol.* 2010; 33:398–407. [PubMed: 19675447]
9. Kruse CA, Cepeda L, Owens B, Johnson SD, Stears J, Lillehei KO. Treatment of recurrent glioma with intracavitary alloreactive cytotoxic T lymphocytes and interleukin-2. *Cancer Immunol Immunother.* 1997; 45:77–87. [PubMed: 9390198]
10. Kruse CA, Beck LT. Artificial-capillary-system development of human alloreactive cytotoxic T-lymphocytes that lyse brain tumours. *Biotechnol Appl Biochem.* 1997; 25:197–205. [PubMed: 9198273]
11. Kruse, CA.; Rubinstein, D. Cytotoxic T lymphocytes reactive to patient major histocompatibility proteins for therapy of recurrent primary brain tumors. In: Liau, LM.; Becker, DP.; Cloughesy, TF.; Bigner, DD., editors. *Brain Tumor Immunotherapy.* Humana Press; Totowa: 2001. p. 149-70.
12. Lampson LA. Interpreting MHC class I expression and class I/class II reciprocity in the CNS: reconciling divergent findings. *Microsc Res Tech.* 1995; 32:267–85. [PubMed: 8573777]
13. Read SB, Kulprathipanja NV, Gomez GG, Paul DB, Winston KR, Robbins JM, et al. Human alloreactive CTL interactions with gliomas and with those having upregulated HLA expression from exogenous IFN-gamma or IFN-gamma gene modification. *J Interferon Cytokine Res.* 2003; 23:379–93. [PubMed: 14511464]
14. Lampson LA, Hickey WF. Monoclonal antibody analysis of MHC expression in human brain biopsies: tissue ranging from “histologically normal” to that showing different levels of glial tumor involvement. *J Immunol.* 1986; 136:4054–62. [PubMed: 2422272]
15. Bigner DD, Bigner SH, Ponten J, Westermarck B, Mahaley MS, Ruoslahti E, et al. Heterogeneity of Genotypic and phenotypic characteristics of fifteen permanent cell lines derived from human gliomas. *J Neuropathol Exp Neurol.* 1981; 40:201–29. [PubMed: 6260907]
16. Kuppner MC, Hamou MF, de Tribolet N. Activation and adhesion molecule expression on lymphoid infiltrates in human glioblastomas. *J Neuroimmunol.* 1990; 29:229–38. [PubMed: 1698816]
17. Kulprathipanja NV, Kruse CA. Microglia phagocytose alloreactive CTL-damaged 9L gliosarcoma cells. *J Neuroimmunol.* 2004; 153:76–82. [PubMed: 15265665]
18. Liu Y, Komohara Y, Domenick N, Ohno M, Ikeura M, Hamilton RL, et al. Expression of antigen processing and presenting molecules in brain metastasis of breast cancer. *Cancer Immunol Immunother.* 2012; 61:789–801. [PubMed: 22065046]
19. Logg CR, Tai CK, Logg A, Anderson WF, Kasahara N. A uniquely stable replication-competent retrovirus vector achieves efficient gene delivery in vitro and in solid tumors. *Hum Gene Ther.* 2001; 12:921–32. [PubMed: 11387057]
20. Tai CK, Wang WJ, Chen TC, Kasahara N. Single-shot, multicycle suicide gene therapy by replication-competent retrovirus vectors achieves long-term survival benefit in experimental glioma. *Mol Ther.* 2005; 12:842–51. [PubMed: 16257382]
21. Wang W, Tai CK, Kershaw AD, Solly SK, Klatzmann D, Kasahara N, et al. Use of replication-competent retroviral vectors in an immunocompetent intracranial glioma model. *Neurosurg Focus.* 2006; 20:E25. [PubMed: 16709031]
22. Wang WJ, Tai CK, Kasahara N, Chen TC. Highly efficient and tumor-restricted gene transfer to malignant gliomas by replication-competent retroviral vectors. *Hum Gene Ther.* 2003; 14:117–27. [PubMed: 12614563]
23. Ostertag D, Amundson KK, Lopez Espinoza F, Martin B, Buckley T, Galvao da Silva AP, et al. Brain tumor eradication and prolonged survival from intratumoral conversion of 5-fluorocytosine to 5-fluorouracil using a nonlytic retroviral replicating vector. *NeuroOncol.* 2012; 14:145–59.

24. Perez OD, Logg CR, Hiraoka K, Diago O, Burnett R, Inagaki A, et al. Design and selection of toca 511 for clinical use: modified retroviral replicating vector with improved stability and gene expression. *Mol Ther.* 2012; 20:1689–98. [PubMed: 22547150]
25. Kikuchi E, Menendez S, Ozu C, Ohori M, Cordon-Cardo C, Logg CR, et al. Highly efficient gene delivery for bladder cancers by intravesically administered replication-competent retroviral vectors. *Clin Cancer Res.* 2007; 13:4511–8. [PubMed: 17671137]
26. Dolecek TA, Propp JM, Stroup NE, Kruchko C. CBTRUS Statistical Report: Primary Brain and Central Nervous System Tumors Diagnosed in the United States in 2005–2009. *NeuroOncol.* 2012; 14 (Suppl 5):v1–v49.
27. Yoneda T, Williams PJ, Hiraga T, Niewolna M, Nishimura R. A bone-seeking clone exhibits different biological properties from the MDA-MB-231 parental human breast cancer cells and a brain-seeking clone in vivo and in vitro. *J Bone Miner Res.* 2001; 16:1486–95. [PubMed: 11499871]
28. Minn AJ, Gupta GP, Siegel PM, Bos PD, Shu W, Giri DD, et al. Genes that mediate breast cancer metastasis to lung. *Nature.* 2005; 436:518–24. [PubMed: 16049480]
29. Tai CK, Logg CR, Park JM, Anderson WF, Press MF, Kasahara N. Antibody-mediated targeting of replication-competent retroviral vectors. *Hum Gene Ther.* 2003; 14:789–802. [PubMed: 12804141]
30. Gomez GG, Kruse CA. Cellular and functional characterization of immunoresistant human glioma cell clones selected with alloreactive cytotoxic T lymphocytes reveals their up-regulated synthesis of biologically active TGF-beta. *J Immunother.* 2007; 30:261–73. [PubMed: 17414317]
31. Garcia S, DiSanto J, Stockinger B. Following the development of a CD4 T cell response in vivo: from activation to memory formation. *Immunity.* 1999; 11:163–71. [PubMed: 10485651]
32. Tomayko MM, Reynolds CP. Determination of subcutaneous tumor size in athymic (nude) mice. *Cancer Chemother Pharmacol.* 1989; 24:148–54. [PubMed: 2544306]
33. Hickey MJ, Malone CC, Erickson KE, Gomez GG, Young EL, Liao LM, et al. Implementing preclinical study findings to protocol design: translational studies with alloreactive CTL for gliomas. *Am J Transl Res.* 2012; 4:114–26. [PubMed: 22347526]
34. Fabre JW. The allogeneic response and tumor immunity. *Nat Med.* 2001; 7:649–52. [PubMed: 11385492]
35. Kranz DM. Incompatible differences: view of an allogeneic pMHC-TCR complex. *Nat Immunol.* 2000; 1:277–8. [PubMed: 11017095]
36. Suchin EJ, Langmuir PB, Palmer E, Sayegh MH, Wells AD, Turka LA. Quantifying the frequency of alloreactive T cells in vivo: new answers to an old question. *J Immunol.* 2001; 166:973–81. [PubMed: 11145675]
37. Hiraoka K, Kimura T, Logg CR, Tai CK, Haga K, Lawson GW, et al. Therapeutic efficacy of replication-competent retrovirus vector-mediated suicide gene therapy in a multifocal colorectal cancer metastasis model. *Cancer Res.* 2007; 67:5345–53. [PubMed: 17545615]
38. Cole C, Qiao J, Kottke T, Diaz RM, Ahmed A, Sanchez-Perez L, et al. Tumor-targeted, systemic delivery of therapeutic viral vectors using hitchhiking on antigen-specific T cells. *Nat Med.* 2005; 11:1073–1081. [PubMed: 16170322]

### Statement of Translational Relevance

Metastasis to the central nervous system is common in advanced breast cancer. With limited treatment options available to patients with metastatic foci, we explored cellular and gene therapy approaches as potential treatments for breast cancer metastatic to brain. This report describes work to indicate the individual, and especially the combined immunogene treatment modalities are effective *in vitro*, and in *in vivo* xenograft models. These novel therapies are well tolerated, brain sparing and provide multiple mechanisms of tumor cell targeted cytotoxicity, including cytotoxic T lymphocyte effector-mediated and chemotherapeutic-mediated cytolysis with suicide vector/prodrug that may be further promoted with bystander effects. Preclinical studies of the individual treatment modalities have warranted their advance to the clinic for treatment of gliomas. Those data and that within this study support accelerated translation of the therapies for treatment of brain metastases.



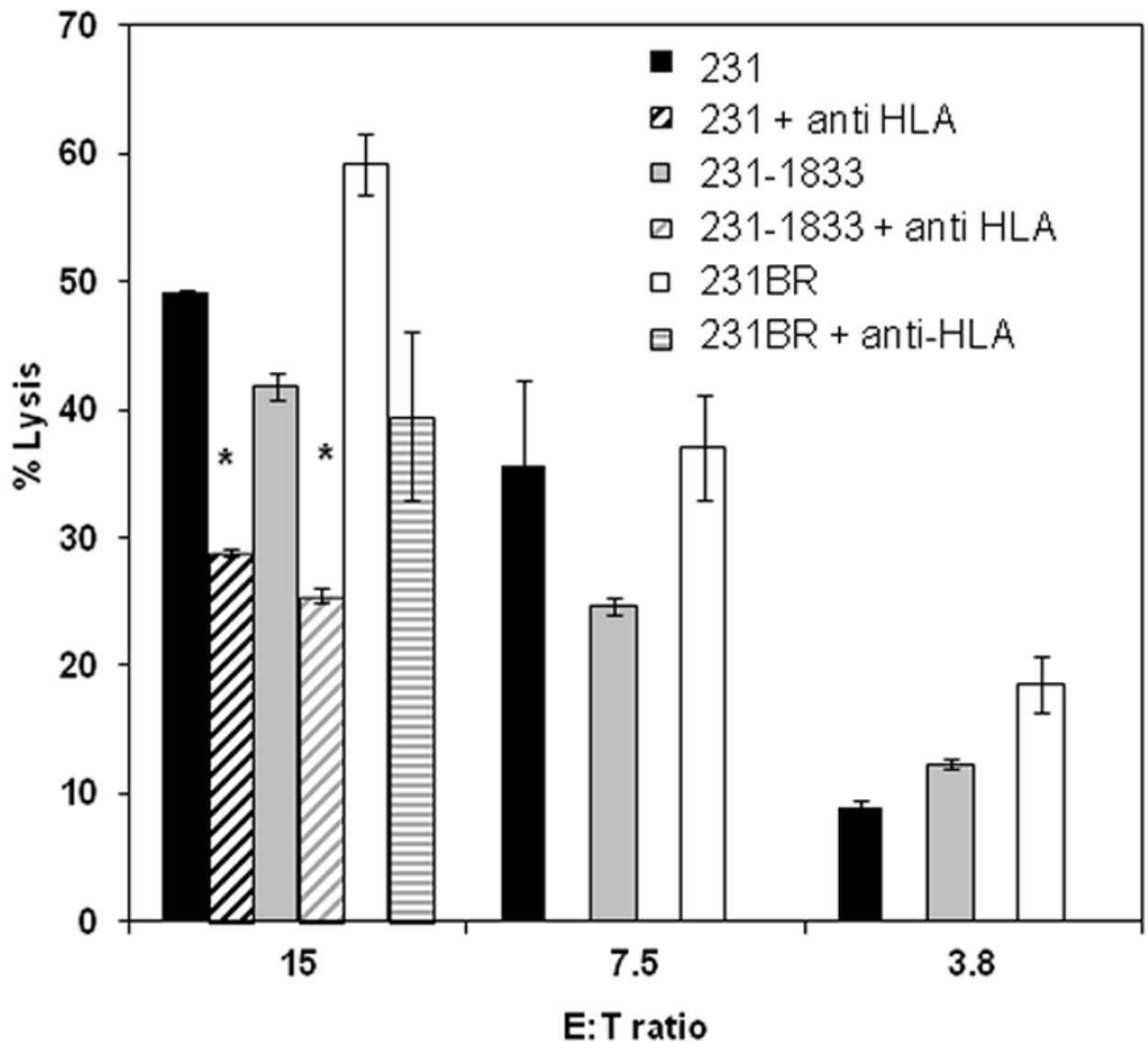


**Figure 1. In vitro cytotoxicity of alloCTL to target cells displaying relevant HLA antigen with alloreactivity demonstrated by inhibition of lysis with anti-HLA-ABC**

4 hr  $^{51}\text{Cr}$ -release assays show that alloCTL generated following one-way MLTR with irradiated stimulator 231 tumor cells are cytotoxic towards the parental 231 cells (black bars) or to metastatic sublines, 231-1833 (gray bars) and 231BR (white bars), at various E:T ratios. HLA-restriction of the cytotoxicity to the three target cell types (231, black angled stripes; 231-1833, gray angled stripes; 231BR, horizontal stripes) was demonstrated (15:1 E:T) by adding antibody to HLA-ABC. Data shown are representative of 3 separate experiments; they are averages of the percentage lysis from triplicate wells + SEM (\*  $p < 0.006$ ).

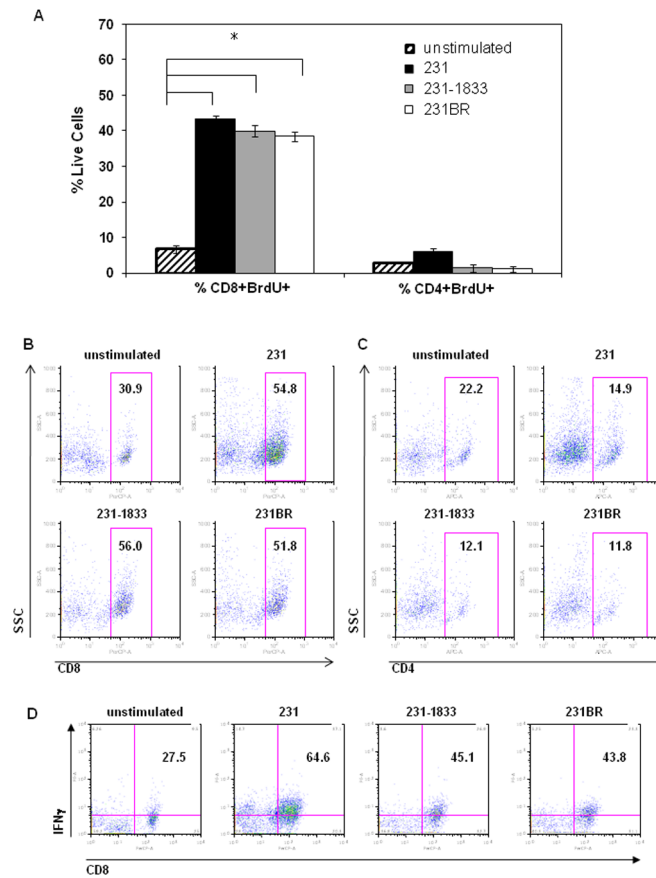


**Figure 2. CD4/CD8 T cell subset proliferation (BrdU incorporation) and IFN $\gamma$  production following alloCTL restimulation**

**A)** BrdU incorporation by CD8+ and CD4+ T cell subsets within alloCTL after their restimulation. Unstimulated (angled stripe), 231 (black bar), 231-1833 (gray bar), 231BR (white bar). The percentages of CD8+ T cells that incorporated BrdU were significantly higher (\*  $p$  0.017) in the CD8+ T cells that were restimulated compared to those that were unstimulated. Representative data from 1 of 3 separate experiments; data are the average percentage of live cells from triplicate wells + SEM. Flow cytometric plots of alloCTL sensitized to 231 and stained for **B)** CD8 or **C)** CD4 72 hr after restimulation with 231, or 231-1833 or 231BR sublines, with unstimulated cells as a control. Data are representative from 1 of 3 separate experiments. **D)** Percentage of CD8+/IFN $\gamma$  + cells alloCTL after restimulation. Representative data are shown from triplicate wells of 1 of 3 separate experiments. Expression of IFN $\gamma$  was significantly higher (\*  $p$  0.017) in CD8+ T cells that were restimulated with 231, 231-1833 and 231BR compared to cells that were unstimulated.

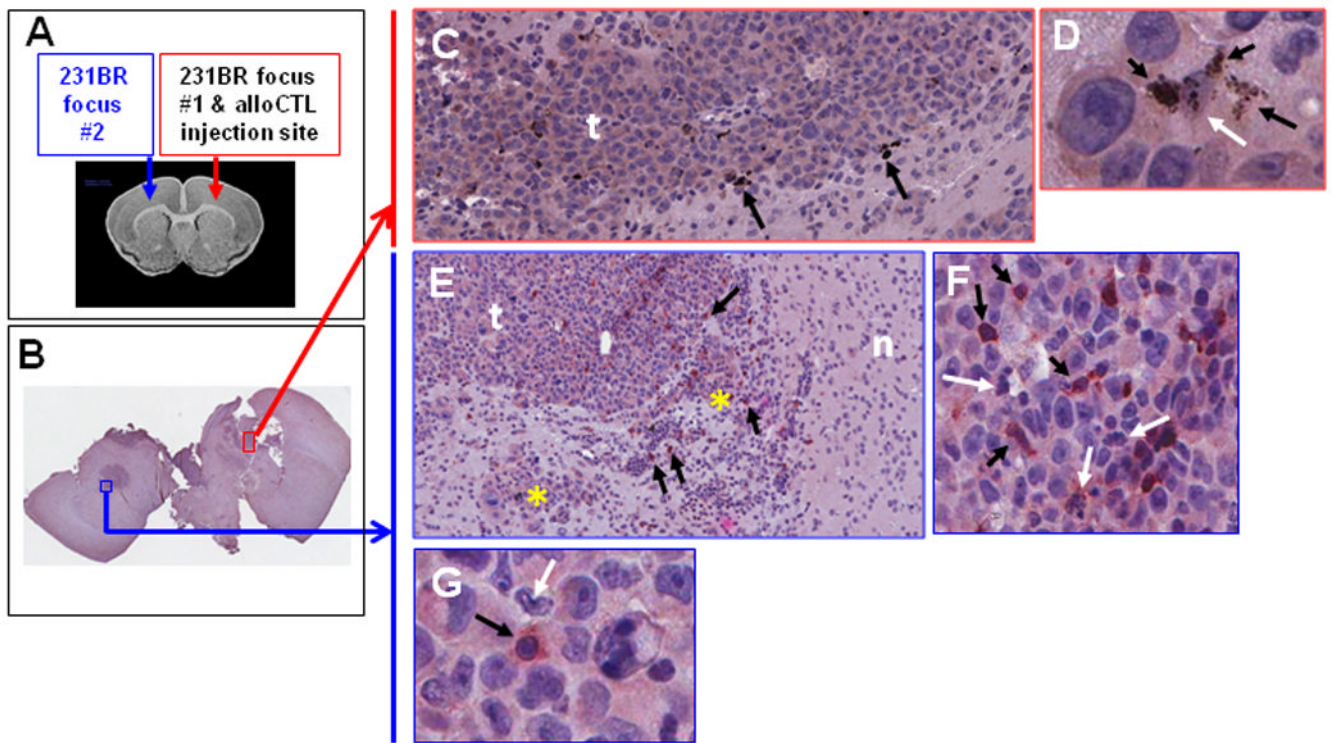


### Figure 3. alloCTL trafficking *in vivo* through and to tumor foci

Brains were collected 6 hr after alloCTL injection into a 3-week established 231BR tumor focus as seen by human anti-CD3 positivity in ipsilateral and contralateral tumor foci within immune incompetent mouse brain. **A)** Coronal brain section schematic of tumor placement and alloCTL at ipsilateral injection site. **B)** Gross coronal brain section that was DAB-immunostained with anti-CD3 that shows two tumor foci (ipsilateral-red and contralateral-blue boxes, respectively). **C)** Low power photomicrograph of rust-colored CD3+ cells (black arrows) in tumor (t) focus #1 and alloCTL instillation site. **D)** Higher power view showing three CD3+ cells in juxtaposition to an apoptotic tumor cell (white arrow). **E–G)** Tumor focus #2 in brain contralateral to alloCTL injection. **E)** Low power photomicrograph shows abundant CD3+ cells (black arrows) primarily within the tumor mass (t) but not in normal brain (n) located in the hemisphere opposite to alloCTL instillation. Yellow asterisks show pockets of tumor cells within Virchow-Robin perivascular spaces. **F)** Intermediate and **G)** High power magnification photomicrographs at that site again show apoptotic tumor cells (white arrows) in proximity to CD3+ cells (black arrows). The brain sections are counterstained with hematoxylin. Representative photomicrographs are shown from 1 of 10 mice; two experiments were analyzed after H&E staining and two experiments after DAB-immunostaining. Bars = 0.8 mm in B, 30  $\mu$ m in C, 8  $\mu$ m in D, 35  $\mu$ m in E, 15  $\mu$ m in F, 10  $\mu$ m in G.

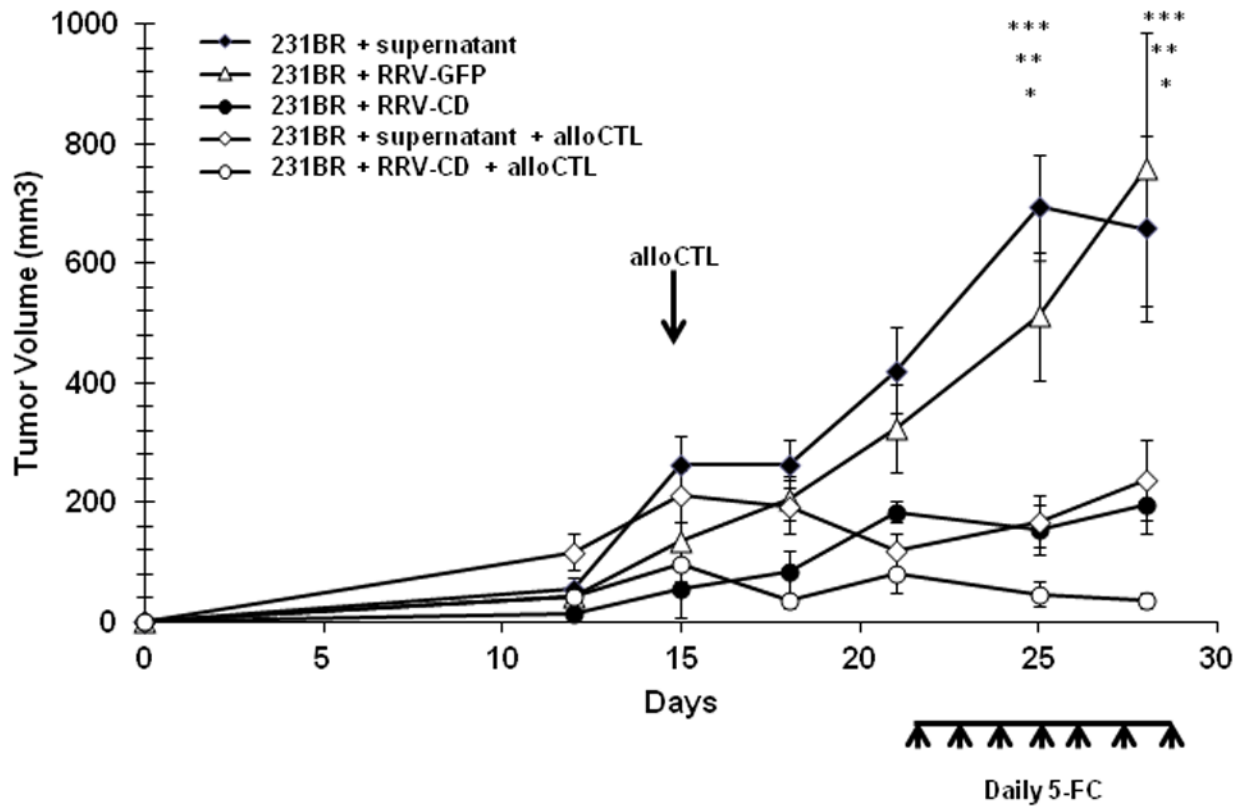


**Figure 4. Subcutaneous tumor volumes to evaluate individual or combined cellular and gene therapy treatment strategies**

*Rag2*<sup>-/-</sup>*γc*<sup>-/-</sup> mice were subcutaneously injected with  $2 \times 10^6$  231BR cells with concentrated RRV-GFP (white triangles), RRV-CD or concentrated non-viral supernate. Tumor growth was allowed to establish for 15 days before some groups received intratumoral injections of  $1.2 \times 10^7$  alloCTL (downward arrow; white circles and white diamonds). All mice were treated with 500mg/kg 5FC i.p. from days 21–27 post subcutaneous tumor injection (upward arrows). Data are represented as the average tumor volume + SEM. Asterisks indicate  $p < 0.017$  by two-way ANOVA with Bonferroni post-tests between mice who received MDA-231BR + concentrated sup (black diamonds) and the following experimental groups: \*, MDA-231BR + concentrated sup + day 15 alloCTL (white diamonds); \*\* MDA-231BR + RRV-CD + day 15 alloCTL (white circles); \*\*\* MDA-231BR + RRV-CD (black circles). Similar findings were obtained from two tumor volumetric experiments; one experiment was a Winn-type assay (n=4 mice/group) and the second experiment shown here was an established tumor assay (n=6 mice/group).

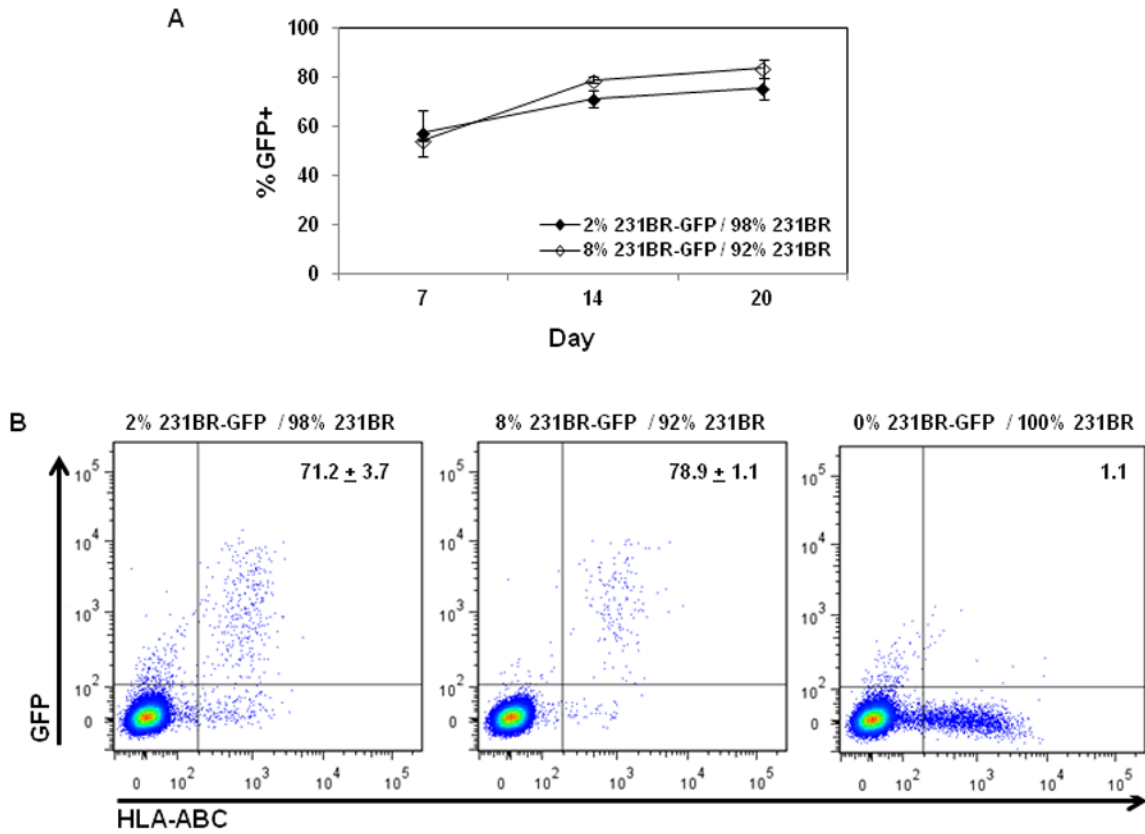


**Figure 5. *In vivo* RRV-GFP spread through intracranial 231BR tumor**

Rag2<sup>-/-</sup>γc<sup>-/-</sup> mice were intracranially injected with a total inoculum of 2 x 10<sup>5</sup> 231BR tumor cells containing either 2% or 8% 231BR-GFP vector producing cells. **A)** Vector spread in nontransduced tumor cells was evaluated at 7, 14 and 20 days post tumor instillation using enzymatically digested tumor cells that stained positive for GFP and were also positive for anti-human HLA, ABC. Data are averages of GFP+/HLA-ABC+ cells from triplicate wells ± SEM. **B)** Representative flow cytometric data from day 14 post tumor instillation demonstrating 71.2 ± 3.7% GFP+ cells from the 2% (left), and 78.9 ± 1.1% from the 8% 231BR-GFP (middle) supplemented populations, respectively. Tumor cells isolated from a mouse intracranially injected with 100% 231BR are shown as a negative control (right). One experiment; n=3 mice/group/timepoint.

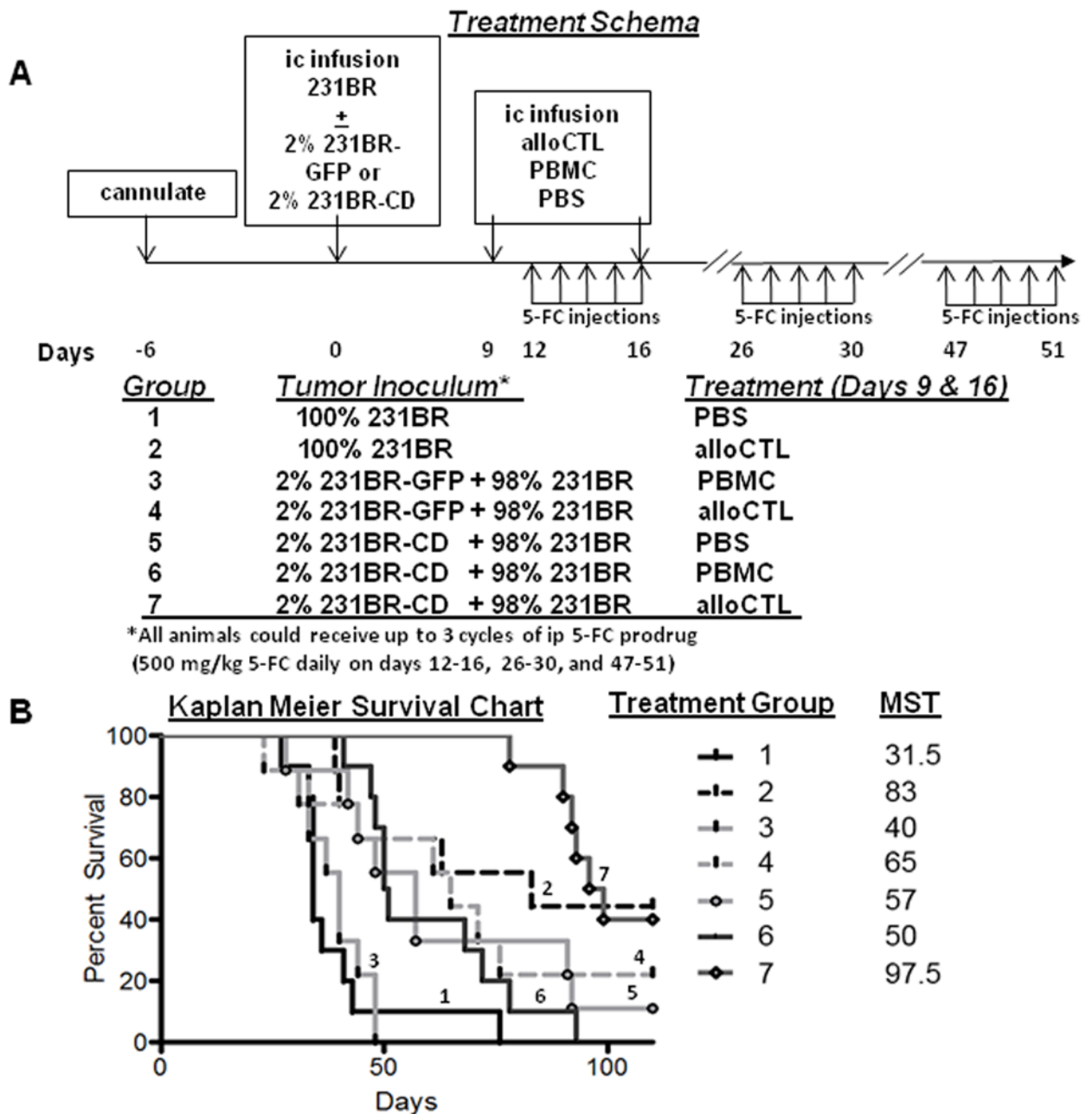


**Figure 6. Immunogene treatment schema, control and experimental treatment groups, Kaplan Meier survival plots with mean survival times**

**A)** The treatment schema along with the 7 control or experimental groups are detailed. Mice were first surgically implanted with cannulas. Six days later they were intracranially infused with either nontransduced 231BR cells or 2%/98% mixtures of RRV-transduced/nontransduced 231BR cells. The transduced 231BR cells had RRV coding for either nontherapeutic GFP marker gene (control) or therapeutic CD gene. alloCTL (therapeutic cells) or PBMC (unstimulated control cells) were infused into the tumor site on days 9 and 16 post-tumor infusion. All animals received the nontoxic prodrug, 5-FC, which was intraperitoneally injected daily for 5 days (one cycle; up to 3 cycles were possible spaced 2–3 weeks apart). Groups 1 and 3 were controls for the suicide gene therapy and cellular

therapy treated groups. The experimental groups testing cellular therapy with alloCTL were groups 2 and 4. The experimental groups testing suicide gene therapy were group 5 and 6. The combination immunogene therapy was group 7. **B)** The Kaplan Meier survival plots along with the median survival times (MST) are shown for all 7 control or experimental groups (n=9–10/group) as observed to day 112 post-tumor injection. Long-term survivors were obtained for all individual or combined cellular and gene therapeutic groups. The p values of significance ( $p < 0.05$ ) calculated by nonparametric Log-Rank (Mantel-Cox) tests were as follows from this singular experiment:

<u>Groups</u>	<u>Treatments</u>	<u>p value</u>
Groups 1,2	PBS vs alloCTL	0.0011
Groups 1,4	PBS vs GFP+alloCTL	0.0365
Groups 3,2	GFP+PBMC vs alloCTL	0.0038
Groups 3,4	GFP+PBMC vs CD+alloCTL	0.0101
Groups 1,5	PBS vs CD	0.0078
Groups 1,6	PBS vs PBMC +CD	0.0051
Groups 3,5	GFP+PBMC vs CD	0.0093
Groups 3,6	GFP+PBMC vs CD+PBMC	0.0004
Groups 1,7	PBS vs alloCTL+CD	0.0001
Groups 3,7	GFP+PBMC vs CD+alloCTL	0.0001

Three separate survival experiments were performed; two pilot studies with n=4–6/group gave similar findings.